Waste Technology (WasTech)
Journal homepage: http://ejournal.undip.ac.id/index.php/wastech
An International Journal

Carbon Quantum Dots (CQds) from Rambutan and Pandan Leaves for Cu^{2+} Detection

Laksmi Dewi Kasmiarno[1], Andini Fikarda[1], Reforny Krisianti Gunawan[1], Isnaeni[2], Supandi[3], Nonni Soraya Sambudi[4,5*]

[1]Chemical Engineering Department, Universitas Pertamina, Simprug, Jakarta Selatan 12220, Indonesia
[2]Research Center for Physics, Group of Applied Laser and Theoretical Physics, LIPI, Tangerang, Indonesia
[3]Department of Pharmacy, Faculty of Pharmacy and Science UHAMKA, Jl. Delima II Klender Jakarta 13460, Indonesia
[4]Chemical Engineering Department, Universiti Teknologi of PETRONAS, Seri Iskandar, Perak 32610, Malaysia
[5]Centre of Urban Resource Sustainability (CUReS), Universiti Teknologi PETRONAS, Seri Iskandar, Perak, 32610, Malaysia
*Corresponding author, E-mail address: soraya.sambudi@utp.edu.my

Abstract - *A facile and eco-friendly process for synthesizing carbon quantum dots (CQDs) was carried out via hydrothermal and microwave treatment using Rambutan and Pandan leaves as carbon sources. The effects of synthesis methods on the optical and physical properties of CQDs, and the sensing activity of CQDs through Cu^{2+} detection are presented in this study. From the analysis, the band-gap energies of CQDs are found to be ranging from 2.52 to 3.51 eV. The CQDs solutions exhibit significant fluorescence property, in which bright cyan fluorescence can be detected under Ultraviolet (UV) light irradiation at a wavelength of around 405 nm. The CQDs synthesized from Pandan and Rambutan leaves using the hydrothermal method show quantum yield (QY) values at around 2.46% and 2.70%, respectively. The FT-IR analysis recorded existing functional groups on the surface of CQDs to be of hydroxyl and carbonyl groups, which can serve as adsorption sites for the detection of Cu2+. Furthermore, this study indicates that CQDs emission from Pandan and Rambutan leaves using hydrothermal method shows the best turn-off behavior when detecting the presence of Cu^{2+} with minimum limit of detection (LoD) as low as 123 µM.*

Keywords *– Carbon Quantum dots (CQDs); leaves; hydrothermal; microwave; copper ions.*

Submission: January 19, 2021 Correction: April 4, 2021 Accepted: April 25, 2021

Doi: http://dx.doi.org/10.14710/wastech.9.1.1-10

[How to cite this article: Kasmiarno, L. D., Fikarda, A., Gunawan, R. K., Isnaeni, Supandi, Sambudi, N. S.. (2021). Carbon Quantum Dots (CQds) from Rambutan and Pandan Leaves for Cu^{2+} Detection. Waste Technology, 9(1), 1-10 doi: http://dx.doi.org/10.14710/wastech.9.1.1-10]

1. Introduction

Toxic heavy metals have been found to inflict dangerous threats to the environment. Based on toxicology, heavy metals can be divided into essential and non-essential heavy metals (Badan POM RI, 2010). Essential heavy metals are heavy metals needed by organisms, but they will cause toxic effects in excessive amounts, such as Zn, Cu, Fe, and Co. Heavy metal pollution is generally originated from various types of waste such as domestic, industrial, agricultural, and mining (Badan POM RI, 2010).

Copper (Cu) as a type of heavy metal is often found in the environment. Its presence is usually in the form of a bivalent ion, $Cu^{2+,}$ which is generally produced by the dye, paper, and oil industries. The process of controlling the release of Cu^{2+} in the aquatic environment is deemed necessary due to its toxicity in the excessive amount, which can cause nervous system disorders, vomiting, cramps, or even death (Fu and Wang, 2011). The existence of copper has been detected in food because of the excessive use of fertilizer and pesticides (Widaningrum, Miskiyah and Suismono, 2016). The Indonesia Institute of Drug and Food Control (BPOM) has determined the maximum copper concentration in fish to be around 20,000 ppb (Priyanto, Dwiyitno and Ariyani, 2008).

There were several methods available for heavy metal ions detection with high accuracy such as atomic absorption spectrometry (AAS), plasma mass spectrometry (PMS), atomic florescence spectrometry (AFS), electrochemical method, and potentiometer (Murugan *et al.*, 2019). Some of these methods were meant to perform sensitivity analyses with high accuracy. However, early on-site detection may be needed before more advanced analysis is performed due to the inability of the equipment. The utilization of quantum dots (QDs) for metal detection has been developed for a long time (Hu *et al.*, 2019), such as for Hg^{2+} (Xie *et al.*, 2019), Fe^{3+} (Jia *et al.*, 2019), and Cu^{2+} (Yingshuai, Zhao and Zhang, 2014).

CQDs as non-metal QDs show unique characteristics such as stable photoluminescence (PL) intensity, good water solubility, inert, and non-toxic (Fu and Wang, 2011) is suitable for metal detection in the aquatic environment. The CQDs are widely applied for photo-catalyst treatment (Fernando *et al.*, 2015), medical diagnosis and imaging (Sachdev and Gopinath, 2015); (Bhamore *et al.*, 2019) (Alam *et al.*, 2015), and transition metals detection (Murugan *et al.*, 2019) (Sachdev and Gopinath, 2015). CQDs have been synthesized using several methods like electrochemical, hydrothermal, acidic oxidation, pyrolysis, and laser ablation. However, some methods have limitations, such as utilizing dangerous chemicals, complex procedures, and numerous purification steps. In this study, the CQDs were synthesized separately using hydrothermal and microwave methods due to the ease, one-step process, and high yield of these methods (Alam *et al.*, 2015; Fernando *et al.*, 2015; Bano *et al.*, 2018; Xie *et al.*, 2019; Yang and Park, 2019).

Synthesis of CQDs using natural materials has become a trend due to the waste-to-advanced material concept, eco-friendliness, and abundant availability in nature. So far, Rambutan and Pandan leave derived—CQDs has not been reported before. However, CQDs have been synthesized successfully using natural materials for heavy metal ions detection, such as using bamboo leaves for Cu^{2+} detection (Yingshuai, Zhao and Zhang, 2014), Enokitake mushroom for detection of Cr^{6+} (Mr *et al.*, 2018), and biomass for Hg^{2+} detection (Xie *et al.*, 2019). In this work, the synthesis of highly fluorescent CQDs from Rambutan and Pandan leaves via hydrothermal and microwave treatment, respectively, was performed for Cu^{2+} detection. The characteristics of CQDs synthesized using hydrothermal and microwave will be compared using UV-Vis spectrophotometry, FTIR analysis and PL spectroscopy.

2. Methodology

2.1 Pre-treatment raw materials

Rambutan and Pandan leaves were washed using aquadest then dried at 90 °C for 6 hours. The dried leaves were grounded and sieved to get the particle size at around 40 µm. Teflon-lined hydrothermal autoclave and microwave were used to synthesize CQDs from dried leaves.

2.2 Synthesis of CQDs using hydrothermal and microwave methods.

Firstly, 150 mg of dried leaves powder were dispersed into 50 mL of aquadest. The leaves were then placed inside teflon-lined autoclave. The autoclave was heated in oven at 200°C for 6 hours for the hydrothermal method. Using the same procedure, the dispersed leaves was placed inside the microwave and irradiated for 30 minutes at 360 Watt. The solution was separated from a larger particle of carbonaceous material using centrifugation at 8,000 rpm for 15 minutes.

2.3 Analytical Method

2.3.1 Characterization of CQDs

The PL and absorption properties of samples were observed using a fluorescence spectrophotometer (Ocean Optics Maya 2000 Pro spectrometer and Picoquant Laser) at wavelength of 405 nm, and UV-Vis spectrophotometer (Ocean Optics Maya 2000 Pro spectrometer). The available functional groups on the samples were recorded and analyzed using a Fourier transform infra-red (FTIR) spectrometer (NicoletTM iS5). QY value was calculated based on established procedure (Lakowicz, 2006) using quinine sulfate 0.1 M H2SO4 as the reference [Q = 0.54].

2.3.2 Detection of the metal ion by CQDs

The fluorescence spectra of CQDs were analyzed in existence and absences of 2 ml Cu^{2+} ions with various concentrations (50 µM, 100 µM, 200 µM, and 400 µM) in 5 ml of CQDs liquid using PL analysis at the exciting wavelength of 405 nm.

3. Result and Discussion

3.1 Physical characteristic of CQDs

The images in Fig. 1 show physical characteristic result of CQDs after the hydrothermal and microwave synthesis using dried Rambutan Leaves (DRL-CQDs), fresh Rambutan Leaves (FRL-CQDs), dried Pandan leaves (DPL-CQDs) and fresh Pandan Leaves (FPL-CQDs). These synthesized CQDs shows different liquid color before and after hydrothermal and microwave treatment, respectively.

Based on Fig. 1a – 1h, all the CQDs products have similar yellowish-brown colors after hydrothermal and microwave treatment. The FRL-CQDs via hydrothermal method tend to have darker brown color than other CQDs samples. The obtained color change indicates that the carbonization has occurred during synthesis. The possible mechanisms for converting leaves into CQDs through hydrothermal method can involve several processes, such as hydrolysis, dehydration, condensation, aromatization, and carbonization (Sahu et al., 2012). The result shows good agreement to Yingshuai et al. experiment that used bamboo leaves as carbon sources and reported the synthesis solution changed into dark brown solution after being heated at 200°C for 6 hours via the hydrothermal method (Yingshuai et al., 2014). Liu et al. also reported that their CQDs product from the grass as precursor obtained yellowish solution after being treated by the hydrothermal process at 180°C for 3 hours (S. Liu et al., 2012). The other experiment from Bano et al. also exhibited a black-brown solution from Tamarindus Indica leaves after hydrothermal treatment for 5 hours at 210 °C (Bano et al., 2018).

Meanwhile, leaves as carbon sources could also transform into CQDs via the microwave method. This method uses electromagnetic energy emitted from microwave irradiation. The electromagnetic energy will be absorbed by the solvent precursor, which is water, for this experiment. Due to the absorbed energy from microwave irradiation, water will cause the CQDs molecules to change their carbon chains' arrangement. Hence, it will produce kinetic energy that generates heat energy for the CQDs carbonization process (Yang & Park, 2019). The CQDs resulted from Rambutan and Pandan Leaves via microwave method show similar physical characteristic to the ones synthesized using hydrothermal method. For instance, Feng et al. reported that CQDs solution from rose petals changed from red to brown solution after continuous heating by microwave oven (Feng et al., 2015). Another study reported by Ramanan et al. also showed the appearance of brownish-black solution from eutrophic algal blooms-derived CQDs after being heated by microwave oven at 600 W for 5 minutes 50 seconds (Ramanan et al., 2016).

3.2 Optical properties of CQDs

The absorbance and fluorescence spectra of CQDs products from each sample are shown in Fig. 2 and 3. Based on the optical absorbance of samples, CQDs have excitation behavior in the wavelength range of 280-330 nm. The peaks in the range of 280 nm – 330 nm might indicate the π-π* transition of C=C bonds in CQDs (Bano et al., 2018). The different surface structures from samples might cause the absorption peak to shift to a longer wavelength. The maximum absorption intensity in the spectrum can be assigned to the amount of CQDs formed (Meng et al., 2019).

This experiment result showed that synthesized CQDs show good agreement to the Gu et al., Yingshuai et al., Kumar et al., Sachdev et al., and Ramanan et al. results, that reported UV-visible absorption spectrum of CQDs are typically shown to have peaked in the ultraviolet area with a tail expanding in the visible area. The absorption of CQDs located in 230-300 nm is generally related to π-π* transition of C=C and another peak located around 310-500 nm is attributed to n-π* transition of C=O (Sachdev & Gopinath, 2015; Kumar et al., 2017; Ramanan et al., 2016; Gu et al., 2016; Yingshuai et al., 2014).

The emission intensity at the excitation wavelength of 405 nm presents that all samples tend to emit visible cyan to light blue color, shown in Fig. 3. According to Fig. 2 (c) and 2 (d), it can be seen that CQDs from both dried-leaves via hydrothermal method have the highest emission peak at 493.73 nm (for Pandan leaves) and 490 nm (for Rambutan leaves), resulting in a bright blue fluorescence of CQDs. The emission intensity was attributed to the surface defects, zigzag sites, and band-gap like the transition of different functional groups present on the surface of CQDs (V. N. Mehta et al., 2015).

The emission color emitted from each sample corresponds to the wavelength range of 430 -570 nm at the blue-green range in the color spectrum (J. Liu et al., 2017). The photoluminescence results resemble the results from previous studies by Ren et al., Bano et al., Yingshuai et al., where maximum emission peak from leaves-derived CQDs have a wavelength range of 405-500 nm with bright blue emission (Ren et al., 2018; Bano et al., 2018; Sachdev & Gopinath, 2015; Yingshuai et al., 2014). The emission intensity graphs indicate that CQDs have different emissive trapped surface states in fluorescence emission. From the previous study, the presence of isolated sp^{-2} clusters with a size less than 3 nm in the carbon-oxygen sp^3 matrix leads to the localization of electron-hole pairs, providing consistent band gaps with blue fluorescence emission (Eda et al., 2010). Besides the size and surface effects, the cyan-blue fluorescence from CQDs samples indicates that the oxygen functional group and electron attract the nitrogen atoms, which contribute to the observed blue shift in the photoluminescence emission (Lin et al., 2015). However, the other emission peaks were found at 677 nm and 671 nm for DRL-CQDs and FRL-CQDs from microwave treatment (Fig. 2 (c)). These peaks indicate that the chlorophyll compounds remained in the samples (Haq, 2019). Nonetheless, the chlorophyll intensity of the samples was not too high compare to the CQDs compound.

To further explore the fluorescent properties of the CQDs products, QY and the relevant factor which affect the emission of CQDs were investigated. The QY calculation is considered as the effectiveness of the light conversion process of absorbed excitation to emission. Obtaining the luminesced CQDs with much higher QY is going to be a major challenge. This requires not only exquisite synthesis strategy but also clarifying the mystery of PL mechanism in CQDs (Zhu et al., 2012). In this work, the highest QY was exhibited by dried Pandan leaves-derived CQDs from the hydrothermal method that reached 2.79% (Table 1).

Table 1. Quantum Yield of Each Sample using Quinine Sulfite as Standard

CQDs Material	Absorption at 405 nm	Quantum Yield (%)
Quinine sulfate	257000	54
DRL- Hydrothermal	56250	2.70
FRL- Hydrothermal	25164	1.26
DRL- Microwave	15554	1.01
FRL- Microwave	10601	0.76
DPL- Hydrothermal	45426	2.79
FPL- Hydrothermal	24388	1.70
DPL- Microwave	12730	0.99
FPL- Microwave	10959	0.87

The shift of emission peaks might occur due to the quantum effect phenomenon. This effect could be caused by different sizes of CQDs or different surface state distribution and functional groups on CQDs (Fu & Wang, 2011). When the particle size gets smaller, the band-gap of a particle will get bigger and require more energy to excite and de-excite electrons at lower wavelengths (De & Karak, 2013). In contrast, the difference in emission intensity from each sample is due to the number of excited particles (De & Karak, 2013).

Another explanation related to the emission peaks was explained by Chakraborty et al. They reported that the generation of electron-hole pairs or excitons are bound to occur when a photon absorbs energy greater than that of the semiconductor band-gap by electrostatic attraction (Chakraborty et al., 2019). The average distance between an electron and the hole is of the order of Bohr radius. Hence, the optical and electrical properties of semiconductor then becomes dependent upon its physical dimensions when its size approaches the Bohr radius (Chakraborty et al., 2019; A. Mehta et al., 2019).

3.3 Band-gap and functional groups

The band-gap result could be a major factor in determining the electrical conductivity of a material. Based on the Tauc plot method, the band-gap energy obtained from the results of analysis varies between 3.51 eV - 2.52 eV. This work shows similarity with the band-gap value calculated from the previous study by Khefacha et al. and Soltani et al. Soltani et al., reported bandgap energy of 2.64 eV for the synthesized CQDs (Soltani et al., 2012). Khefacha et al. identified the result of band-gap energy to be around 2.36 eV (Khéfacha et al., 2016).

Table 1. Band gap energy of each sample

CQDs Material	Band Gap Energy
DRL- Hydrothermal	2.52 eV
FRL- Hydrothermal	2.98 eV
DRL- Microwave	3.01 eV
FRL- Microwave	3.51 eV
DPL- Hydrothermal	2.83 eV
FPL- Hydrothermal	3.30 eV
DPL- Microwave	3.36 eV
FPL- Microwave	3.42 eV

The FTIR spectra of CQDs are shown in Fig. 4. The absorption peaks of CQDs for each sample from Rambutan leaves recorded from 3323.62 cm^{-1} to 3333.61 cm^{-1} were assigned to hydroxyl and amine group (Wang & Hu, 2014), and stretching vibration of C=O is found between 1634.20 cm-1 and 1635.42 cm^{-1} (Nguyen et al., 2015). CQDs from Pandan leaves show similar results, which peaks around 3310.83 cm^{-1} to 3313.07 cm^{-1} are assigned to O-H and N-H vibrations in the surface of CQDs (Wang & Hu, 2014). The other peaks at 1635.46 cm^{-1} to 1646.55 cm^{-1} are ascribed to C=O bonds in CQDs surface state (Nguyen et al., 2015). The analysis result of FTIR spectra confirm successful synthesis of CQDs. These absorption bands of functional groups show similarity with previous study by Liu et al, which O-H bonds and N-H bonds appear at absorption bands of 3100-3450 cm^{-1}. Also for other functional groups in the absorption band of 1600-1707 cm^{-1} are assigned to C=O bond (W. Liu et al., 2017).

3.4 Detection of Copper (Cu^{2+})

The measurement of copper (Cu^{2+}) ions detection by CQDs is shown in Fig. 5. It shows that CQDs could detect Cu^{2+} ions with high sensitivity. The emission intensity from each sample decreases gradually as the Cu^{2+} ion concentration increased. The significant PL-quenching occurs after the addition of Cu^{2+} ion. CQDs from each sample has carboxyl and carbonyl atom on its surface, hence the efficient binding affinity with vacant d-orbital of Cu^{2+} and carbonyl in CQDs can refer to its natural selectivity in this sensing system. At the same time, the -OH atoms give the electron pair to vacant d-orbital of Cu^{2+} ions and non-radiative electron transfer (Murugan et al., 2019; (Kumar *et al.*, 2017)].

The CQDs sensitivity can be observed from a significant decrease in emission intensity when the CQDs respond to the analyte (Cu^{2+}). This study shows the same agreement as to the previous study by Liu et al. in using grass-derived CQDs as biosensors. The addition of metal ions corresponds to the decreasing of CQDs emission intensity (Liu *et al.*, 2012). The results show that along with the addition of Cu^{2+} ion concentration, the emission intensity decreases significantly. It proves that the CQDs obtained are very sensitive to copper metal ions (Liu *et al.*, 2012). Yingshuai et al., also reported that the highest emission sensitivity obtained from CQDs could be due to high QY (Yingshuai, Zhao and Zhang, 2014). Based on the experiment, the CQDs from DRL - hydrothermal and DPL- hydrothermal show the most sensitive behavior to the effect of the copper addition, thus the CQDs can be used for further development as detection agents for hazardous metal.

Based on the fluorescence intensity spectra before and after adding a Cu2+ solution into CQDs, LoD results were obtained using the Stern–Volmer equation, as shown in Table 3. The result showed various LoD values for each sample with the lowest LoD was recorded by DRL-CQDs synthesized via the hydrothermal method with the value of 123.67 μM (Table 3). The LoD results obtained were relatively large due to the concentration range used, but the results obtained showed that the results of the CQDs synthesized in this study, especially DRL-CQDs was very sensitive to detect the presence of Cu^{2+} ions, hence the CQDs are suitable to be applied as a biosensor to detect the presence of copper metal.

Table 2. LoD of each CQDs sample

CQDs Synthetic Method	DRL	FRL	DPL	FPL
	LoD (μM)			
Hydrothermal	123.67	346.12	282.898	247.006
Microwave	189.52	355	233.164	800.642

4. Conclusion

This work used Rambutan and Pandan leaves as carbon sources to synthesize CQDs through hydrothermal and microwave methods. The synthesized CQDs solution generated cyan fluorescence under ultraviolet light irradiation at a wavelength of 405 nm. The analysis of CQDs indicates the existence of C=O and C=C bonds, band-gap varies from 3.42 eV to 2.52 eV, and QY from 0.87 to 2.79%. Furthermore, the CQDs from dried leaves using hydrothermal treatment have the highest intensity compared to other samples, at the maximum emission of 493.73 nm. Moreover, the result obtained showed DRL-CQDs to be more effective for the detection of Cu^{2+} ions with high sensitivity.

Acknowledgment

This work is supported by UTP-UHAMKA collaborative research grant with cost center 015ME0-143.

References

Alam, A.-M. et al. (2015) ‘Synthesis of carbon quantum dots from cabbage with down- and up-conversion photoluminescence properties: excellent imaging agent for biomedical applications’, Green Chemistry, 17(7), pp. 3791–3797.

Badan POM RI (2010) Mengenal Logam Beracun.

Bano, D. et al. (2018) ‘Green synthesis of fluorescent carbon quantum dots for the detection of mercury (II) and glutathione’, New Journal of Chemistry, 42.

Bhamore, J. R. et al. (2019) ‘Green synthesis of multi-color emissive carbon dots from Manilkara zapota fruits for bioimaging of bacterial and fungal cells’, Journal of Photochemistry and Photobiology. B, Biology, 191, pp. 150–155.

Fernando, K. A. S. et al. (2015) ‘Carbon quantum dots and applications in photocatalytic energy conversion’, ACS applied materials & interfaces, 7(16), pp. 8363–8376.

Fu, F. and Wang, Q. (2011) ‘Removal of heavy metal ions from wastewaters: a review’, Journal of Environmental Management, 92(3), pp. 407–418.

Hu, L. et al. (2019) ‘Luminescence Change of CdS and CdSe Quantum Dots on a Ag Film’, ACS Omega, 4(10), pp. 14193–14201.

Jia, J. et al. (2019) ‘Highly luminescent N-doped carbon dots from black soya beans for free radical scavenging, Fe3+ sensing and cellular imaging’, Spectrochimica Acta. Part A, Molecular and Biomolecular Spectroscopy, 211, pp. 363–372.

Kumar, A. et al. (2017) ‘Green synthesis of carbon dots from Ocimum sanctum for effective fluorescent sensing of Pb2+ ions and live cell imaging’, Sensors and Actuators B: Chemical, 242, pp. 679–686.

Liu, S. et al. (2012) ‘Hydrothermal Treatment of Grass: A Low-Cost, Green Route to Nitrogen-Doped, Carbon-Rich, Photoluminescent Polymer Nanodots as an Effective Fluorescent Sensing Platform for Label-Free Detection of Cu(II) Ions’, Advanced Materials, 24(15), pp. 2037–2041.

Mr, P. et al. (2018) ‘Highly fluorescent carbon dots from enokitake mushroom as multi-faceted optical nanomaterials for Cr6+ and VOC detection and imaging applications’, Applied Surface Science, 453, pp. 192–203.

Murugan, N. et al. (2019) ‘Green synthesis of fluorescent carbon quantum dots from Eleusine coracana and their application as a fluorescence “turn-off” sensor probe for selective detection of Cu^{2+}’, Applied Surface Science, 476, pp. 468–480.

Priyanto, N., Dwiyitno, D. and Ariyani, F. (2008) ‘Kandungan Logam Berat (Hg, Pb, Cd, dan Cu) Pada Ikan, Air, dan Sedimen Di Waduk Cirata, Jawa Barat’, Jurnal Pascapanen dan Bioteknologi Kelautan dan Perikanan, 3(1), pp. 69–78.

Sachdev, A. and Gopinath, P. (2015) ‘Green synthesis of multifunctional carbon dots from coriander leaves and their potential application as antioxidants, sensors and bioimaging agents’, The Analyst, 140(12), pp. 4260–4269.

Widaningrum, nFN, Miskiyah, nFN and Suismono, nFN (2016) ‘Bahaya Kontaminasi Logam Berat Dalam Sayuran dan Alternatif Pencegahan Cemarannya’, Buletin Teknologi Pasca Panen, 3(1), pp. 16–27.

Xie et al. (2019) ‘Green Hydrothermal Synthesis of N-doped Carbon Dots from Biomass Highland Barley for the Detection of Hg^{2+}’, Sensors, 19, p. 3169.

Yang, G. and Park, S.-J. (2019) ‘Conventional and Microwave Hydrothermal Synthesis and Application of Functional Materials: A Review’, Materials, 12, p. 1177.

Yingshuai, L., Zhao, Y. N. and Zhang, Y. (2014) ‘One-step green synthesized fluorescent carbon nanodots from bamboo leaves for copper(II) ion detection’, Sensors and Actuators B: Chemical, 196, pp. 647–652.

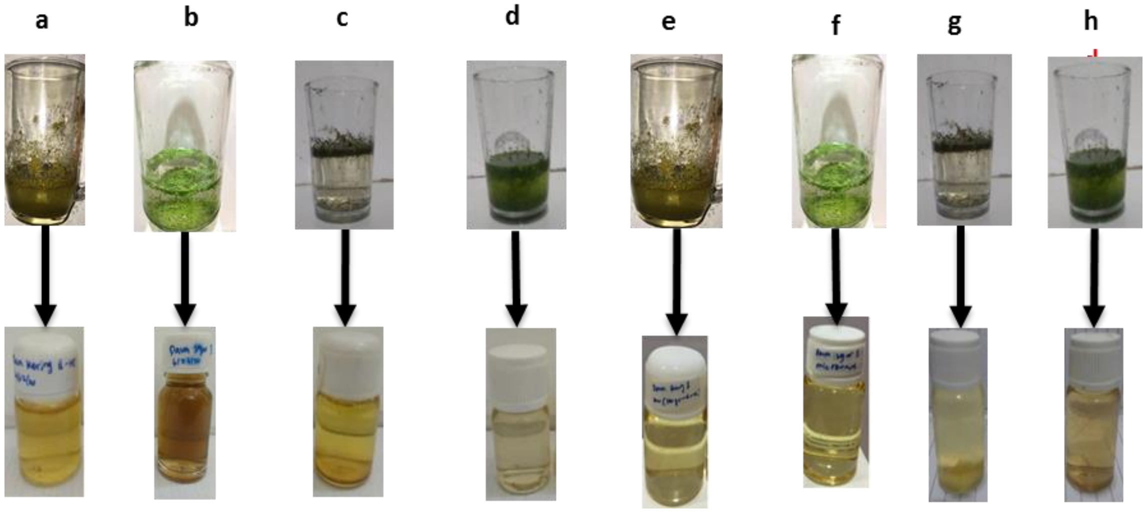

Figure 1. The physical appearance of CQDs from (a) DRL-CQDs-Hydrothermal, (b) FRL-CQDs-Hydrothermal, (c) DPL-CQDs-Hydrothermal, (d) FPL-CQDs-Hydrothermal, (e) DRL-CQDs-Microwave, (f) FRL-CQDs- Microwave, (g) DPL-CQDs-Microwave, and (h) FPL-CQDs-Microwave

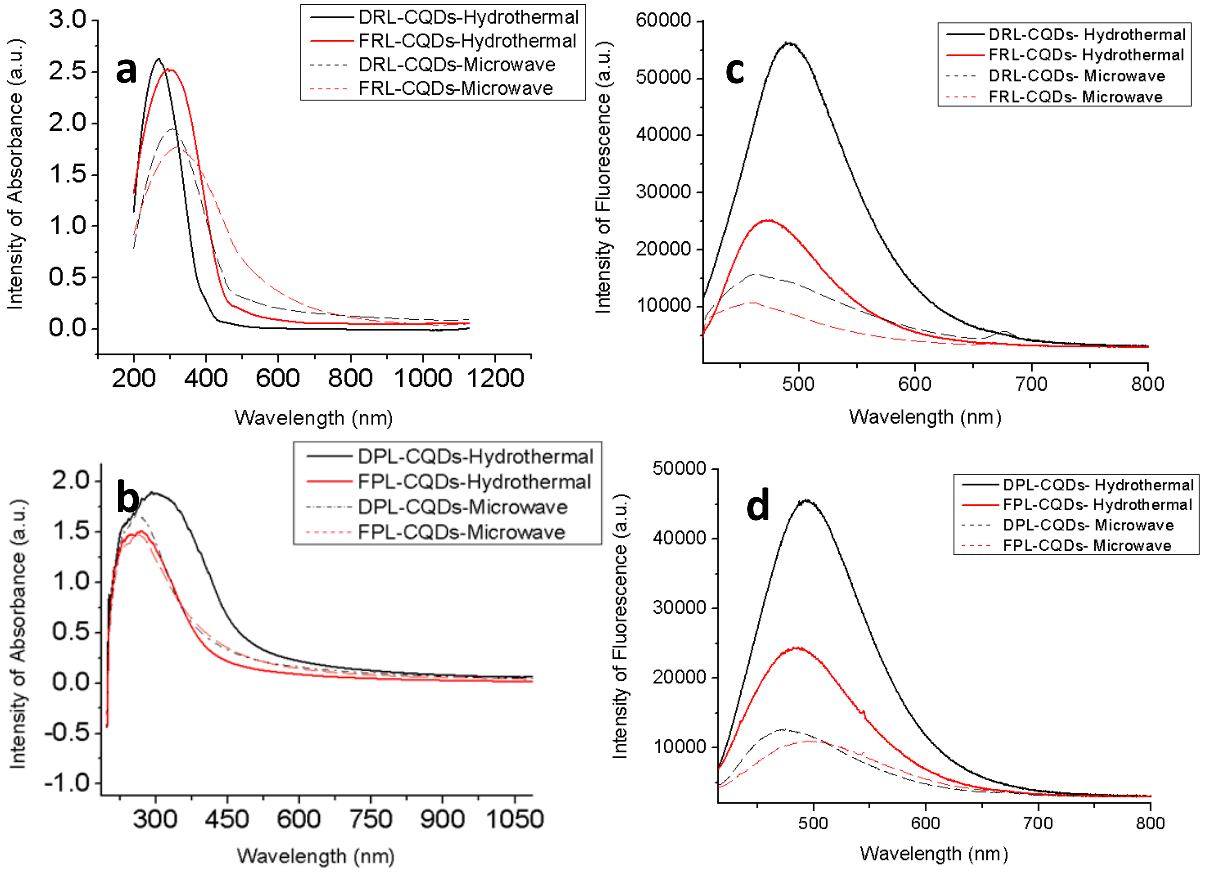

Figure 2. UV-vis spectrum of CQDs from (a) Rambutan leaves and (b) Pandan leaves ; Fluorescense spectra of CQDs from (c) Rambutan leaves and (d) Pandan Leaves

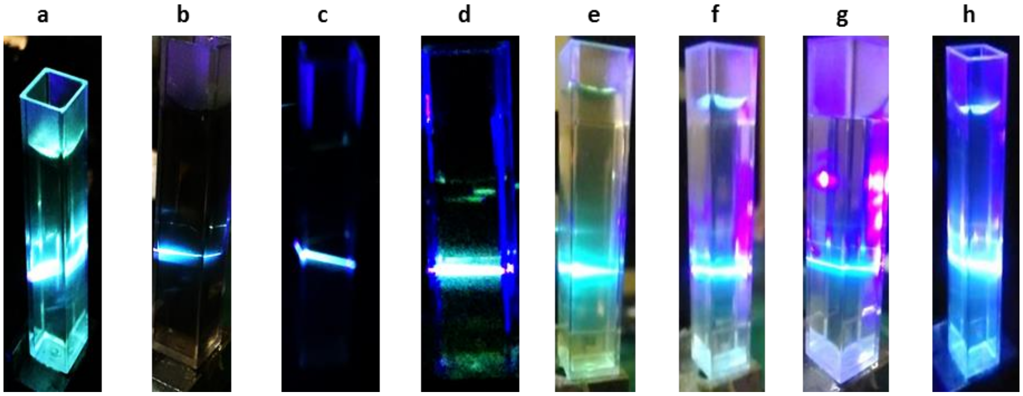

Figure 3. The physical appearance of CQDs emission from (a) DRL-CQDs-Hydrothermal, (b) FRL-CQDs-Hydrothermal, (c) DRL-CQDs-Microwave, (d) FRL-CQDs- Microwave, (e) DPL-CQDs-Hydrothermal, (f) FPL-CQDs-Hydrothermal, (g) DPL-CQDs-Microwave, (h) FPL-CQDs- Microwave

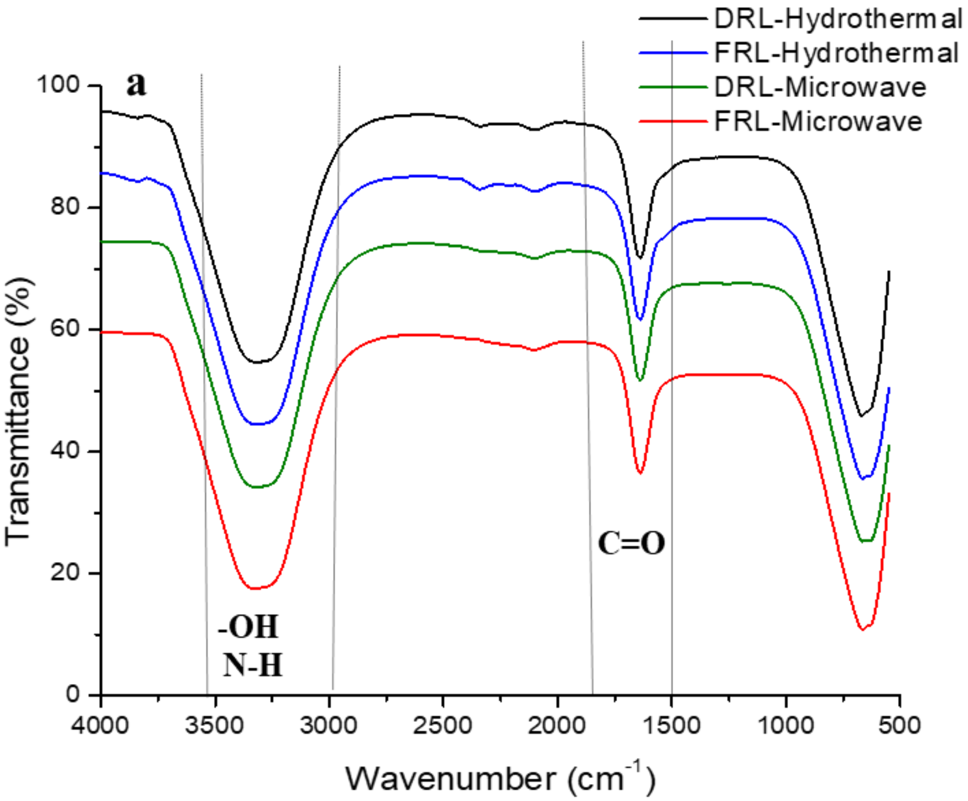

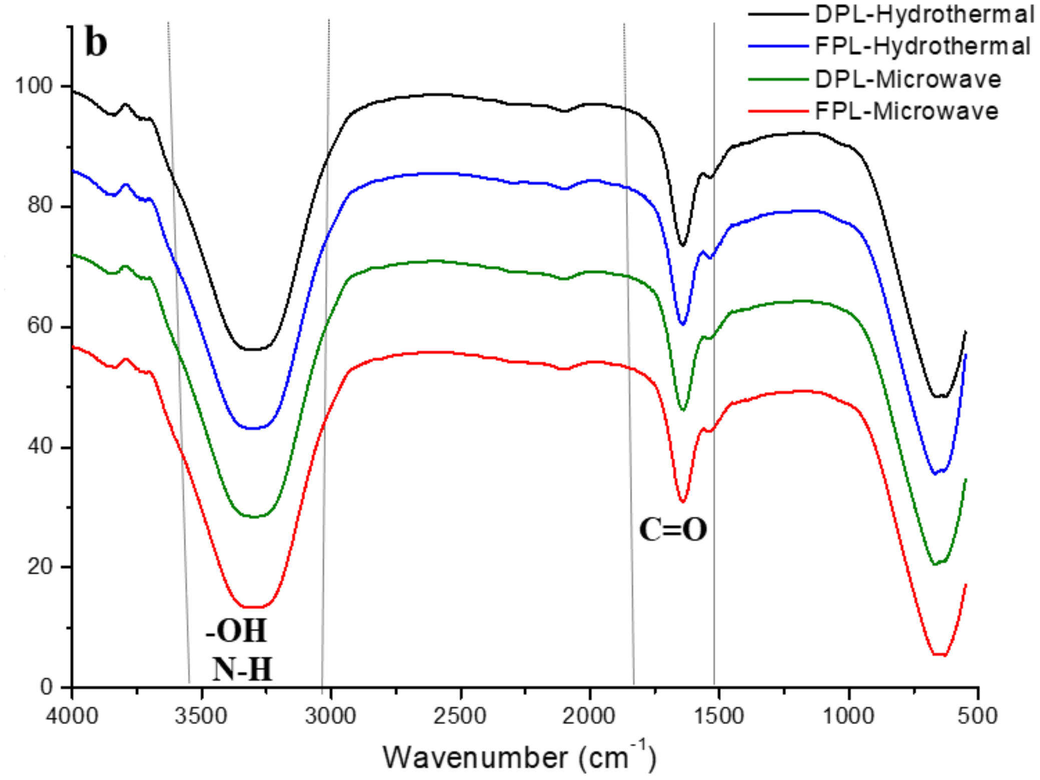

Figure 4. FT-IR spectra of CQDs from (a) Rambutan leaves and (b) Pandan leaves

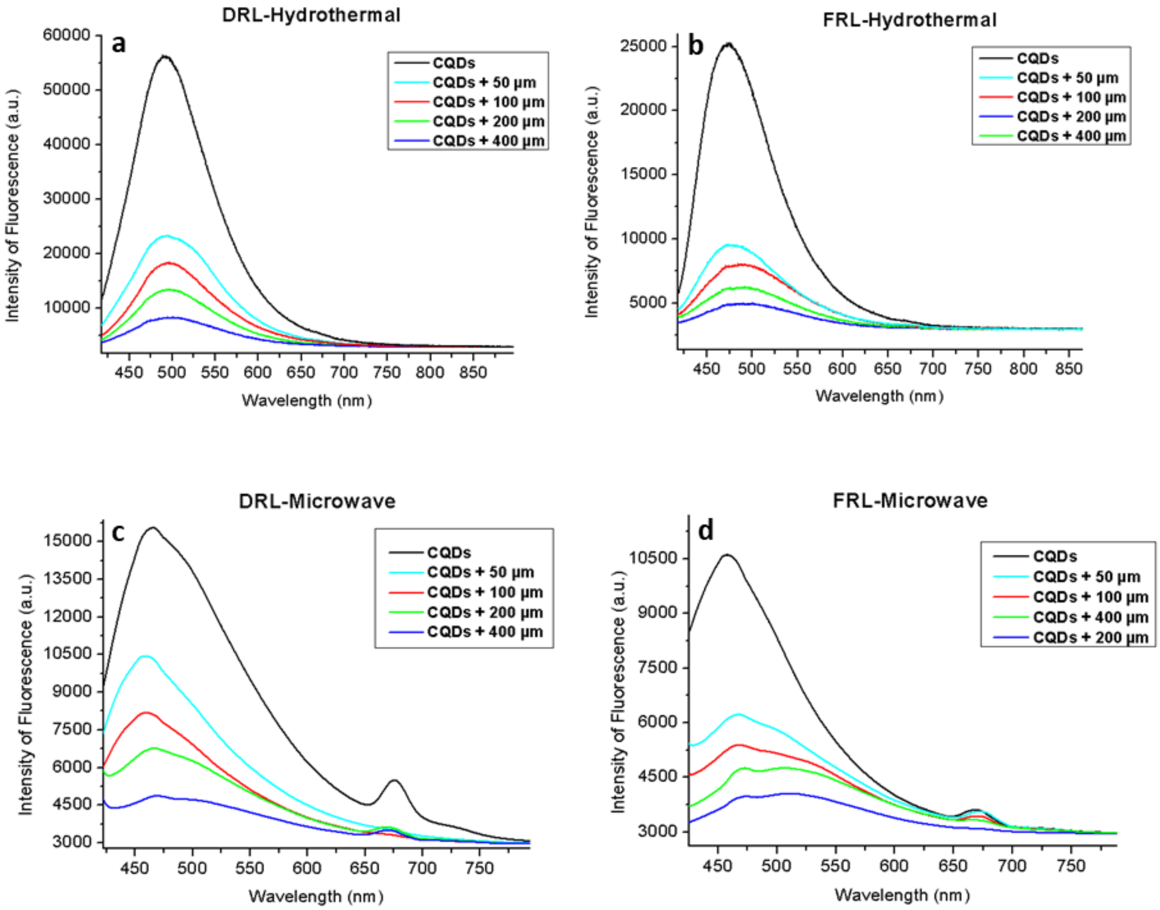
DRL-Hydrothermal
a
Intensity of Fluorescence (a.u.)
60000
50000
40000
30000
20000
10000
450 500 550 600 650 700 750 800 850
Wavelength (nm)
CQDs
CQDs + 50 µm
CQDs + 100 µm
CQDs + 200 µm
CQDs + 400 µm
FRL-Hydrothermal
b
Intensity of Fluorescence (a.u.)
25000
20000
15000
10000
5000
450 500 550 600 650 700 750 800 850
Wavelength (nm)
CQDs
CQDs + 50 µm
CQDs + 100 µm
CQDs + 200 µm
CQDs + 400 µm
DRL-Microwave
c
Intensity of Fluorescence (a.u.)
15000
13500
12000
10500
9000
7500
6000
4500
3000
450 500 550 600 650 700 750
Wavelength (nm)
CQDs
CQDs + 50 µm
CQDs + 100 µm
CQDs + 200 µm
CQDs + 400 µm
FRL-Microwave
d
Intensity of Fluorescence (a.u.)
10500
9000
7500
6000
4500
3000
450 500 550 600 650 700 750
Wavelength (nm)
CQDs
CQDs + 50 µm
CQDs + 100 µm
CQDs + 400 µm
CQDs + 200 µm

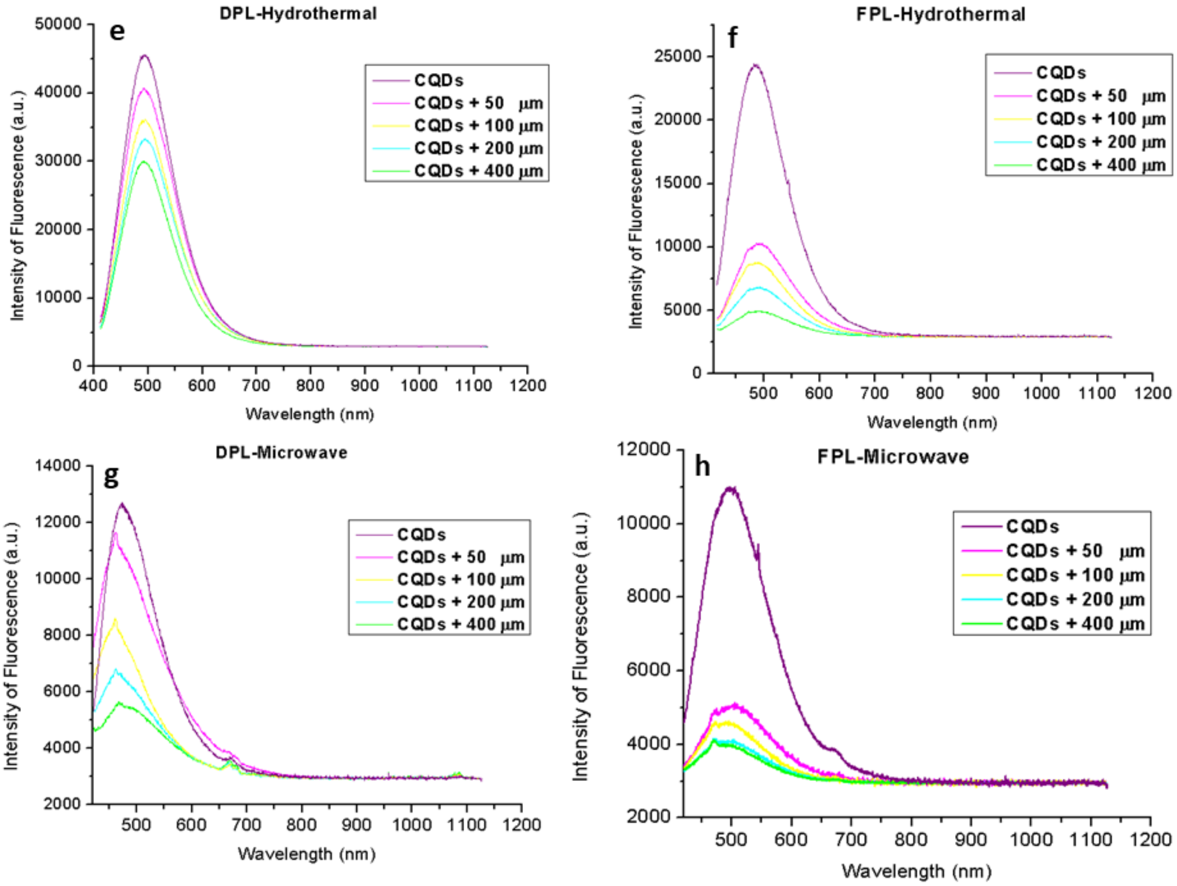

Figure 5. Fluorescence spectra of CQDs with different concentration of Cu2+ from (a) DRL-CQDs - hydrothermal, (b) FRL-CQDs – hydrothermal, (c) DRL-CQDs – microwave, (d) FRL-CQDs – microwave, (e) DPL-CQDs - hydrothermal, (f) FPL-CQDs – hydrothermal, (g) DPL-CQDs – microwave, and (h) FPL-CQDs – microwave.